Turk J Chem
26 (2002) , 59 – 76.

Determination of Manganese and Iron in Magmatic Rocks After Ultrasonic Leaching by flame AAS*

M. Hikmet ÖZKAN, Mehmet AKÇAY
Department of Chemistry, Cumhuriyet University,
58140, Sivas-TURKEY
e-mail: hozkan@cumhuriyet.edu.tr

Received 10.10.2000

An alternative sample preparation method has been developed for destructive analysis of magmatic rock sample. The method simply included the crushing, HF treatment and 1% HCl leaching steps of the rock samples under ultrasonic effects. There is no need to exhaust all of the sample through the operation. A reproducible and representative, partial recovery of an analyte was expected in a procedural sequences consisting of strictly defined steps. The changes in analyte recoveries were investigated by sample grain size, sample mass, applied ultrasonic power and sonication time. The optimum recovery conditions were examined. In addition, the kinetics of the dissolution under ultrasonic effects were studied. It was observed that the process followed second order kinetics. The accuracy of the ultrasonic leaching method (C_{ULM}) was tested by application on standard reference material (SRM) and a recovery rate was defined as $K_1 = C_{ULM}/C_{SRM}$. Another recovery rate, K_2, was also defined according to the result of the conventional dissolution method (CDM), that is, $K_2 = C_{ULM}/C_{CDM}$. The accuracy and the precision of the method are comparable with those of the conventional methods;

$91.3\% < K_{1,Mn} < 109.1\%$ and $88.9\% < K_{2,Mn} < 109.1\%$ and

$86.2\% < K_{1,Fe} < 98.9\%$ and $88.9\% < K_{2,Fe} < 107.3\%$

Key Words: Ultrasonic metal leaching, partial leaching, magmatic rocks, AAS

Introduction

Chemical analysis of the geological materials have been conventionally performed by two different methods[1]. One of them is known as the destructive method, and involves UV-VIS, AAS, ICP-AES or MS and NAA. The other one is known as the non- destructive method, or the XRF method. The conventional sample preparation techniques have some serious disadvantages. Many of the techniques used for analysis of geological materials require a sample the dissolution step prior to the measurement step. In fact, frequently, the dissolution step is the most time consuming one in the entire analysis. The sample preparation is frequently the most time consuming and a major potential source of error in any geochemical analysis. In addition, there is

*This paper has beed presented at MBCAC III (3rd Mediterranean Basin Conference on Analytical Chemistry) 4-9 June, 2000 Antalya-Turkey

excess acid consumption in the techniques[1−5]. Despite advances in instrumentation and microcomputer technology, many sample preparation practices are based on nineteenth-century technologies. Furthermore, there is a serious contamination risk with these procedures. Sample preparation steps are frequently the main source of errors in an overall analysis. An ideal dissolution technique should be economical, simple, effective and selective (for interference problems) and require minimum solvent usage. In general, partial dissolution of an analyte from a solid sample is not reproducible and total dissolution seems to be the right choice. However, although quantitative leaching of analyte from a solid sample is not possible, a technique in which a representative portion of the sample can be abstracted that reflects the real composition of the corresponding solid material may be proposed, and we might have enough supporting evidence for this case[6−8];

- A rock sample can be crushed into certain grain sizes which represent the whole rock without any fractionation
- The grain sized rock samples can be partially dissolved using the same chemical treatment or a series of similar treatments with reproducible results (they can be leached).
- Once an analyte is dissolved, its deposition on solid residue and adsorption into a solid surface can be prevented (e.g. by ultrasonication). When a solid mass is exposed to ultrasonic effects, it interacts with the pores of the solid and prevents the deposition of dissolved ions on it. When speed of procedure, reproducibility and solvent consumption are considered, ultrasonic leaching has some advantages over traditional methods[9−11].

The ultrasonic leaching method (ULM) is thought to be an alternative method to conventional total dissolution techniques.

High recoveries of organics have been reported from granular activated carbon[12], sediment[13], fly ash[14], biological materials[15], atmospheric particulate[16] and geological samples[17−19] analysed by ULM, in a much shorter time than is required for other extraction procedures. Similar results may also be expected for labile (physically bound) metal fractions in atmospheric particulate and on bio-collector sprouts, from a study of the physical and chemical effects of ultrasonication[20−22].

The kinetics of partial dissolution have also been investigated. Dissolution kinetics can be written as

$$dS/dt = k(S_{\max} - S)^2 \tag{1}$$

where dS/dt is the dissolution rate, k is the dissolution constant, S_{max} is the maximum amount of soluble material, and S is the amount of solvent material at t. Since the S-t plot is a hyperbole and the dissolution kinetics are predicted to be second order kinetics, Equation (1) should be

$$t/S = A + Bt \tag{2}$$

and should give a linear plot. A is $1/(dS/dt)_0$, B is $1/S_{max}$. When the t/S is plotted against t, a linear function is obtained. Dissolution should follow second order kinetics. r_i(initial dissolution rate) and S_{max} are obtained from the slope and intercept of this graph (t/S-t)[23−26].

It is possible that the advantages of a reproducible partial dissolution method are greater than its disadvantages as a sample preparation procedure.

The objective of this is the investigation of the possibility of obtaining a portion of a rock sample by ULM that reflects the real composition of the sample experimentally and statistically. The conditions of the procedure were optimised for grain size, sample amount, ultrasonication period and ultrasonic power.

Experimental

The rock sample

The magmatic rock sample was obtained from Cumhuriyet University Engineering Faculty Laboratories in Sivas, Turkey. The sample, which was used through this study, was defined as quartz-syenite by the mentioned laboratories[27].

Crushing, sieving and fractionating

Firstly, the superficially weathered parts of rock sample were removed by using a geological hammer. After that, the rock sample was crushed with a Fritsch-Pulverizette type jaw-crusher, with iron and steel jaws, to obtain suitable grain sizes. All these samples comminution (size-reduction) methods have been tested and recommendede by Muller[28], who explained that there is no iron contamination in geological samples due to the already high content of iron, attaining up to 4-5% weight rather than some ppm or ppb levels. For this purpose, the samples were put into a jaw-crusher with a jaw distance of 0.5 cm. The sieving of these roughly crushed rock samples was performed with an Endecotts Octagon-200 model shaker including suitable sieves (see Table 1). The sieving procedure was completed with a shaking rate of 7 for 10 minutes, which is established as the standard sieving condition for intensive igneous rock samples, i.e., quartz syenite, at the Crushing, Grinding and Sieving Laboratory of the Department of Geological Engineering of Cumhuriyet University. The rock sample was fractionated into five sample grain sizes and described in detail in Table 1.

Table 1. Sample grain size, sieve pore size and sieve pore range

Sample grain size no	Sieve pore numbers, mm	Sieve pore range, mm
5	0.425	-0.425+0.250
4	0.250	-0.250+0.106
3	0.106	-0.106+0.063
2	0.063	-0.063+0.038
1	0.038	-0.038+0.000

A total of 720 test solutions were prepared having six different masses (0.0500, 0.1000, 0.2000, 0.3000, 0.4000 and 0.5000 g) and for three different sonication powers (minimum ultrasonic power, medium ultrasonic power and maximum ultrasonic power) and eight different sonication times (5, 10, 15, 20, 30, 40, 50 and 60 minutes) for each grain size.

Softening step

It is known that the studied rock sample has 70% SiO_2[27] and stoichiometrically this amount of silica could be removed with 2.0 cm^3 of concentrated HF (approximately 38%). 25 cm^3 HDPE (high density polyethylene) beakers were treated with blank HF (Merck, Darmstadt, Germany), dried and weighed (after a few treatments). After this pretreatment the weight of the beakers varied by ± 0.0002-0.0008. Then rock

samples were placed into the beakers, and 2.0 cm^3 HF was added and they were dried on a hot plate at 55^oC until dryness and the mass losses (mainly SiO_2) of the samples were determined. The effects of HF amount, HF concentration, sample grain size and sample mass on the procedure of silica removing were also investigated.

Dissolution by ULM

The residue from the silica removing procedure was placed in a 120.0 cm^3 glass beaker, 25.0 cm^3 of 1% HCl (Merck, Darmstadt, Germany) was added and the beakers were kept in an ultrasonic bath, NEY 300 model (50-60 kHz), for leaching. Leaching solutions were centrifuged at 5000 rpm for 10 minutes to separate the residue and solutions were filtered using Whatman 41 filtration paper. 1.0 cm^3 of 1% La^{3+}(for improved atomisation efficiency in AAS analysis) and 1.0 cm^3 concentrated HCl added samples were made up to 50.0 cm^3 with 1% HCl solution and kept in a LDPE (low density polyethylene) bottle for analysis.

Determination of elements

The leaching solutions were analysed for determination of Mn and Fe by flame atomic absorption spectrophotometer (FAAS-UNICAM 929 model) using the standard addition and calibration curve techniques. Standard addition techniques were used to test possible interferences. There were no significant interference effects. Therefore, the calibration curve technique was used in whole analyses. Air-acetylene flame was used for determination of the elements. The calibration curves were prepared using certified standard reference materials for the two elements[29] The calibration ranges were 0.2-3.5 mgL^{-1} for Mn and 1-10 mgL^{-1} for Fe. For matching the dynamic range of the calibration curves, the samples were diluted by a factor of 1/10, 1/50, or 1/100 with 1% HCl, as appropriate, to expected levels of the elements before the determinations. The elements concentrations were obtained as the mean of three readings which provided less than 2% of the relative standard deviation (RSD %).

Results and Discussion

Silica removal by HF

First, the silica content of each sample was removed using concentrated HF and the required minimum HF amount was determined. For example, 0.2000 g portions of samples of grain size 1 was placed in HDPE beakers and 2.0, 4.0, 8.0, 16.0, and 20.0 cm^3 HF was added to the beakers respectively. The previously described softening procedure was followed. The procedure was repeated five times and the average mass losses obtained ($\bar{x}$) are given in Table 2.

Table 2. Mass losses with HF amount (grain size 1 and 0.2000 g sample).

Process no	HF, cm^3	$\bar{x}$, g	Mass loss, %	RSD, %
1	2	0.0833	41.65	0.7
2	4	0.0825	41.25	0.7
3	8	0.0830	41.50	0.7
4	16	0.0835	41.75	0.8
5	20	0.0829	41.45	0.9

As can be seen from Table 2, silica removal is not affected by increasing HF, and the calculated volume (2.0 cm^3) is sufficient for the removal of silica, and hence 2.0 cm^3 of concentrated HF was used for all removing during the study.

The series of experiments was also carried out to test whether mass loss affected grain size. 0.2000 g portions of samples in the five different grain sizes (see Table 1) were taken, 2.0 $cm^3$of HF was added and silica losses were by determined by application of the procedure described above. The results of five replicates are given in Table 3.

Table 3. Mass losses with sample grain size (0.2000 g sample)

Particle size no	HF, cm^3	$\bar{x}$, g	Mass loss, %	RSD, %
1	2	0.0833	41.65	0.7
2	2	0.0860	43.00	0.9
3	2	0.0880	44.47	1.0
4	2	0.0897	45.04	1.4
5	2	0.0910	45.53	0.9

According to the data in Table 3, mass loss (silica removal) increased with grain size (from 41.65% to 45.53%) and 2.0 cm^3 of HF was still sufficient for all size ranges. But it should be indicated that despite the fact that 2.0 cm^3 of HF is sufficient for maximum silica removal, this volume did not give aqueous solution with high sample mass (e.g. 0.5000). Therefore a dilution step was modified rather than using more HF. The gradual dilution steps and water volumes added are given in Table 4 for grain size 1 and 0.2000 g of sample mass.

Table 4. Mass losses (silica removal) with HF dilution (grain size 1 and 0.2000 g sample)

Process no	(HF+water), cm^3	$\bar{x}$, g	Mass loss, %	RSD, %
1	2+1	0.0839	41.95	1.0
2	2+2	0.0835	41.75	1.1
3	2+3	0.0765	38.25	1.2
4	2+3.5	0.0489	24.25	1.8

While addition of 1.0 cm^3 and 2.0 cm^3 of water did not show any significant change, a sharp decrease was observed with more dilutions. Therefore only 2.0 cm^3 of water could be used for dilution. Under these circumstances, repeated dissolution (five replications) using 2.0 cm^3 of HF and 2.0 cm^3 of water were carried out for all particle sizes (0.2000 g and grain size 1-5) and the results are given in Table 5.

Table 5. Mass losses with sample grain size in diluted HF solution (0.2000 g sample)

Grain size no	(HF+water), cm^3	$\bar{x}$, g	Mass loss, %	RSD, %
1	2+2	0.0835	41.75	1.0
2	2+2	0.0862	43.10	0.9
3	2+2	0.0866	44.30	1.2
4	2+2	0.0896	44.80	1.3
5	2+2	0.0906	45.30	1.3

Although the mass losses (silica removal) increased with grain size in Table 5, these results are approximately the same as those in Table 3. Under the light of these findings 2.0 cm^3 of HF + 2.0 cm^3 of water was used for all silica removal experiments.

Initially, 720 aliquots of the same rock samples were prepared for five particle sizes and six masses (for example 0.0500-0.500 g of size 1, 0.0500-0.5000 g of size 2 and so on) at 3 different ultrasonic powers and 8 different leaching periods. Mass losses were determined for each sample and the results were compared by ANOVA significance test[23]. Silica removal with sample mass and particle size are given in Table 6.

Table 6. Silica removal ($\bar{x}$) with six sample masses for five sample grain sizes.

Grain size no#	Sample mass#, g	$\bar{x}$, g	RSD, %
1	0.0500	43.84 ***	2.8
1	0.1000	41.90 *	1.9
1	0.2000	41.54 *	1.7
1	0.3000	42.50 ***	1.8
1	0.4000	44.51 ***	3.6
1	0.5000	45.41 ****	2.6
2	0.0500	42.23 **	2.5
2	0.1000	41.52 *	1.8
2	0.2000	42.83 **	1.8
2	0.3000	44.63 ***	1.5
2	0.4000	44.83 ***	1.7
2	0.5000	45.41****	1.4
3	0.0500	44.38 *	1.8
3	0.1000	43.88 *	1.3
3	0.2000	44.95 **	1.4
3	0.3000	45.79 ***	1.4
3	0.4000	46.26 ***	0.7
3	0.5000	46.57****	1.2
4	0.0500	44.24 *	1.9
4	0.1000	46.25 **	1.9
4	0.2000	45.82 **	1.6
4	0.3000	47.00 ***	1.5
4	0.4000	47.40 ****	2.2
4	0.5000	46.68 **	4.3
5	0.0500	45.68 *	2.4
5	0.1000	46.07 *	2.5
5	0.2000	45.96 *	1.8
5	0.3000	47.14 **	1.7
5	0.4000	48.22 ***	0.9
5	0.5000	45.76 *	2.2

24 equal samples for each mass and grain size

The rock sample studied is a granitoid particle sized silica consisting mainly of mineralogical components (quartz, feldspath, amphibole, biotite, etc.) varying from 2 to 5 mm. However, some very small particles (called accessory minerals) and some oxide and sulphur compounds (called opaque minerals) may also be present in the structure. The quantitative amount of both accessory minerals and opaque minerals will decrease with increasing particle size, and the silica amount is expected to be high. As supported by our findings, a high silica amount was observed with increasing particle size. This significant variance is shown

in Table 6 and is indicated by asterisks (*), as determined by the ANOVA significance test (for P=0.05 and N=24). Silica removal differences between the sample masses with the same number of asterisks are the result of random errors for each particle size.

Ultrasonic power (USP) and sonication period used for leaching process

The ultrasonic bath (NEY 300 model, 50-60 kHz) used in this study has eight different power scales and the power ranges were defined as follows:

first scale: minimum ultrasonic power (min USP).

fourth scale: medium ultrasonic power (med. USP).

eighth scale: maximum ultrasonic power (max USP).

24 equal samples for each grain size and sample mass (total 720 samples) were prepared and subsamples which contained 8 equal samples were grouped. Each of the 8 samples were subjected to the ultrasonic treatment for 5, 10, 15, 20, 30, 40, 50 and 60 minutes at minimum, medium and maximum ultrasonic power individually (see Table 6).

Solubility of Manganese and Iron with ULM

The effects of sonication period, sample mass, grain size and ultrasonic power on ultrasonic leaching are considered in the following sections:

The effect of sonication period

The solubility of manganese and iron of grain size 1 and max USP with sample mass and sonication period is given Figures 1a and 1b respectively. The oxides of the elements will be given as percentages in all figures and tables.

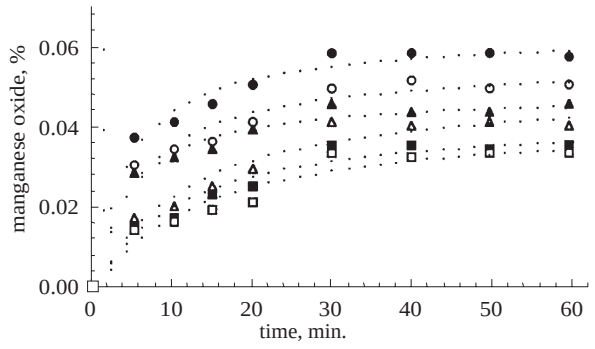

Figure 1a. The change in manganese levels (manganese oxide %) by sample mass and sonication time (grain size 1 and maximum USP)
•; 0.0500 g, ◯; 0.1000 g, ▲; 0.2000 g, Δ; 0.3000 g, ■; 0.4000 g, □; 0.5000 g, ·; theoretical curve.

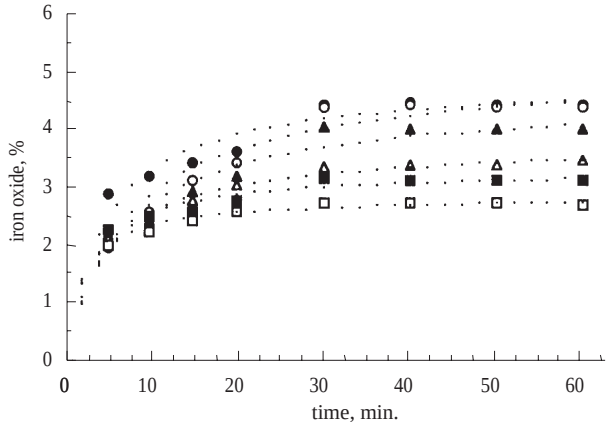

Figure 1b. The change in iron levels (iron oxide %) by sample mass and sonication time (grain size 1 and max USP)
•; 0.0500 g, ◯; 0.1000 g, ▲; 0.2000 g, Δ; 0.3000 g, ■; 0.4000 g, □; 0.5000 g, ·; theoretical curve

The determined manganese oxide and iron oxide (t Fe_2O_3 represents total iron oxide as ferric iron) for the entire mass range (0.0500-0.5000 g) was increased by sonication period in first 30 minutes and then remained constant. However, the best recovery was observed with 0.0500 g of sample mass (minimum recovery at 0.5000 g of sample mass). The constant solubilities for both oxides at 30, 40, 50 and 60 minutes for each sample were used for reproducibility tests. Similar results were observed for other sample sizes and ultrasonic powers.

When the solubility values were plotted against sonication time, the hyperbolic curves were obtained (see Figs.1a and 1b). Therefore it was assumed that the dissolution process should follow the second-order kinetics law. The t/S v t graphs were obtained to prove our assumption and Figures 2a and 2b were obtained for Mn and Fe respectively.

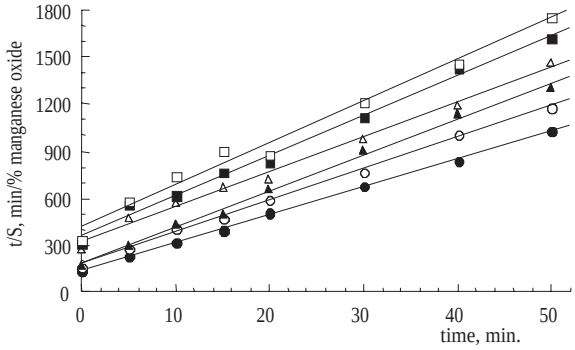

Figure 2a. t/S v t plot of manganese oxide (grain size 1 and maximum USP)
•; 0.0500 g, ◯; 0.1000 g, ▲; 0.2000 g, Δ; 0.3000 g, ■; 0.4000 g, □; 0.5000 g,

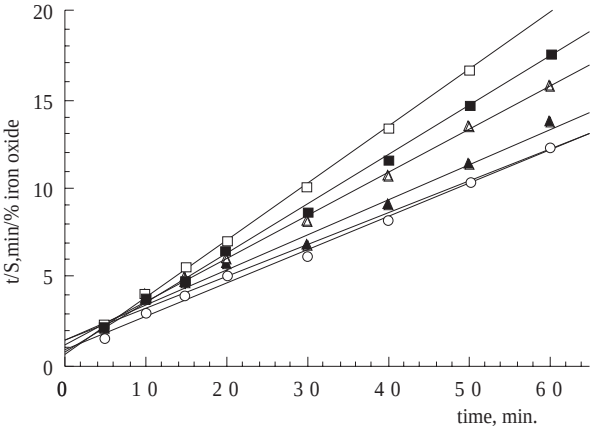

Figure 2b. t/S v t plot of iron oxide (grain size 1 and maximum USP)
•; 0.0500 g, ◯; 0.1000 g, ▲; 0.2000 g, Δ; 0.3000 g, ■; 0.4000 g, □; 0.5000 g,

As can be seen from these figures, a linear increase wes observed, and it was concluded that dissolution process follows the second-order kinetics law. The corresponding r_i and S_{max} values were determined from the slopes and intercepts of these linear plots respectively. The calculated r_i and S_{max} values were plotted against sample mass and are shown in Figures 3a and 3b.

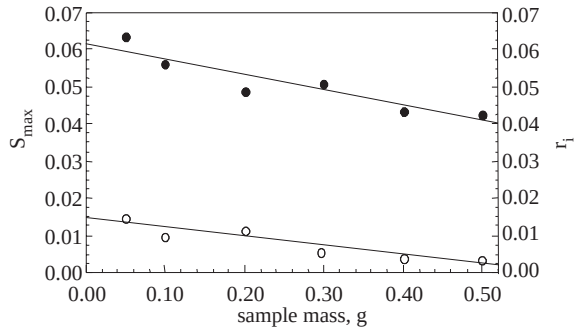

Figure 3a. The change in the values of S_{max} and r_i of manganese oxide with sample mass (grain size 1 and max USP)
•; S_{max} (% manganese oxide / g sample), ◯; r_i(% manganese oxide /min g sample)

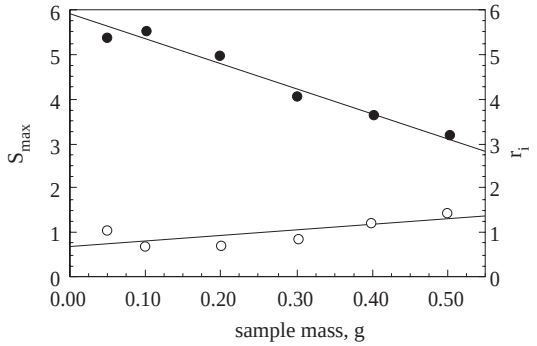

Figure 3b. The change in the values of S_{max} and r_i of iron oxide with sample mass (grain size 1 and max USP)
•; S_{max} (% iron oxide / g sample), ◯; r_i(% iron oxide /min g sample)

Both of these figures show that S_{max} significantly decreased with increasing sample mass. However, initial dissolution rates inhibited different behaviour. While r_i decreased with sample mass for manganese, it remained nearly constant for iron.

The solubilities of Mn and Fe (for 0.0500 g sample mass and maximum USP) by grain size and sonication time are shown in Figures 4a and 4b.

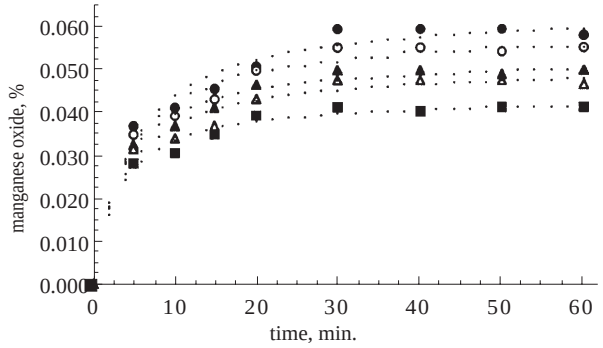

Figure 4a. The change in manganese levels by grain size and sonication time (0.0500 g sample mass and maximum ultrasonic power)
•; grain size 1., ◯; grain size 2., ▲; grain size 3., Δ; grain size 4., ■; grain size 5. ·; theoretical curve

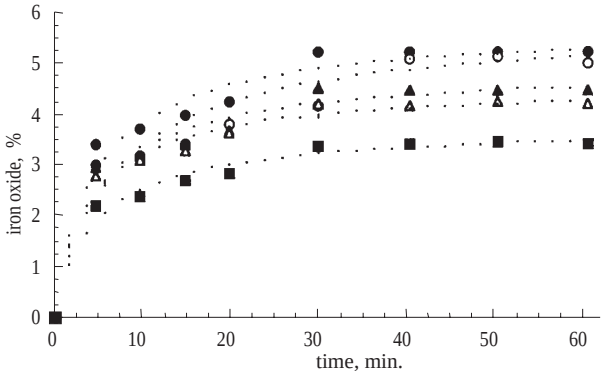

Figure 4b. The change in iron levels by grain size 1 and sonication time (0.0500 g sample mass and maximum ultrasonic power)
•; grain size 1., ◯; grain size 2., ▲; grain size 3., Δ; grain size 4., ■; grain size 5. ·; theoretical curve

The curves of the manganese oxide and iron oxide percentages against the sonication period exhibited similar behaviours. A linear increase in the first 30 minutes was observed, and then the percentage remained constant for all sample grain sizes at max USP for 0.0500 g sample mass.

The linear dissolution graphs were obtained from hyperbolic curves (see 4a and 4b) and are shown in Figures 5a and 5b.

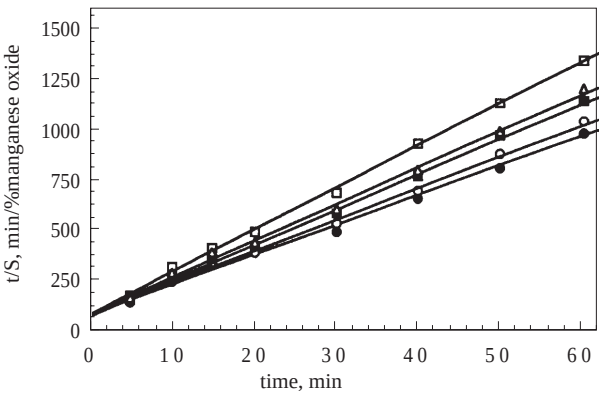

Figure 5a. t/S v t plot of manganese oxide (in max USP and for 0.0500 g sample mass)
•; grain size 1., ◯; grain size 2., ▲; grain size 3., Δ; grain size 4., ■; grain size 5.

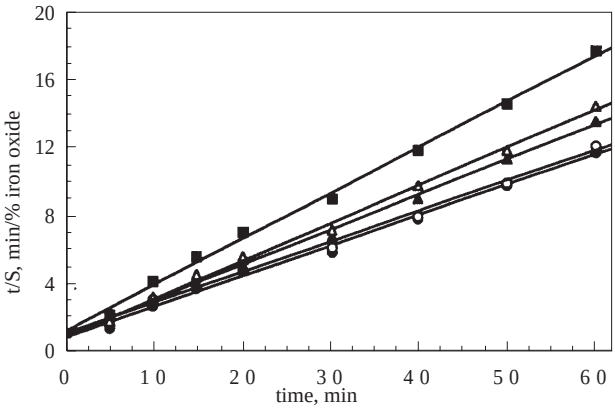

Figure 5b. t/S v t plot of iron oxide (in max USP and for 0.0500 g sample mass)
•; grain size 1., ◯; grain size 2., ▲; grain size 3., Δ; grain size 4., ■; grain size 5.

Again, the calculated r_i and S_{max} values were plotted against sieve pore size and are shown in Figures 6a and 6b.

As can be seen, while r_i values remained constant, S_{max} values decreased linearly with increasing sieve pore size.

Figures 7a and 7b illustrated the changes in solubility for Mn and Fe respectively with sonication time at minimum, medium and maximum ultrasonic power for samples with the same grain size, 1, and a constant mass of 0.0500 g.

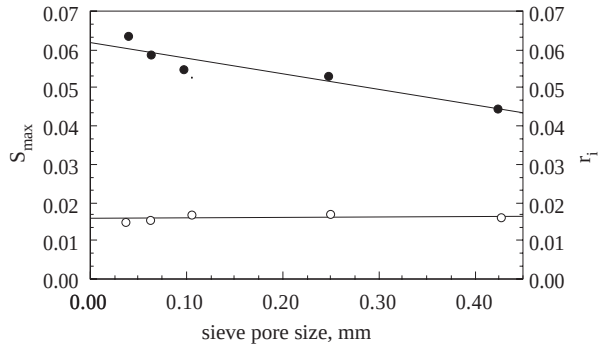

Figure 6a. The change in the values of S_{max} and r_i of manganese oxide with sieve pore size (in max USP and for 0.0500 g sample mass)
•; S_{max}(% manganese oxide / g sample), ◯; r_i(% manganese oxide /min g sample)

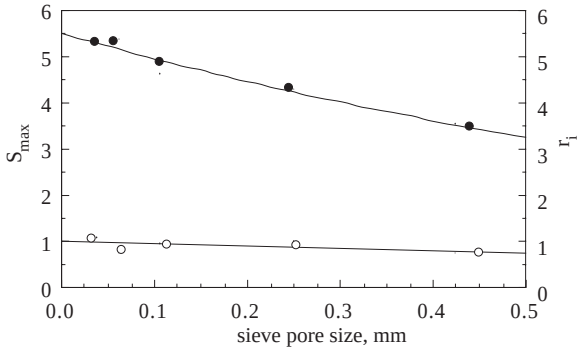

Figure 6b. The change in the values of S_{max} and r_i of iron oxide with sieve pore size (in max USP and for 0.0500 g sample mass)
•; S_{max}(% iron oxide / g sample), ◯; r_i(% iron oxide /min g sample)

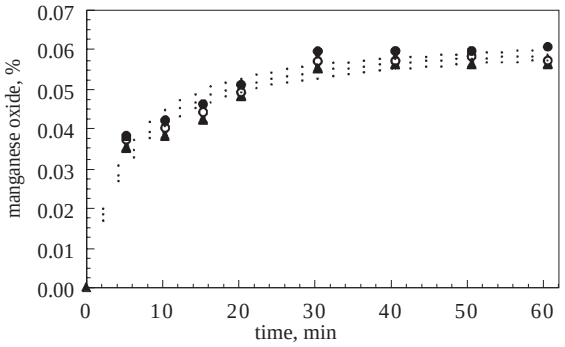

Figure 7a. The change in manganese oxide solubility with USP and sonication time (for samples grain size 1 and mass 0.0500 g)
•; maximum USP, ◯ ; medium USP, ▲; minimum USP

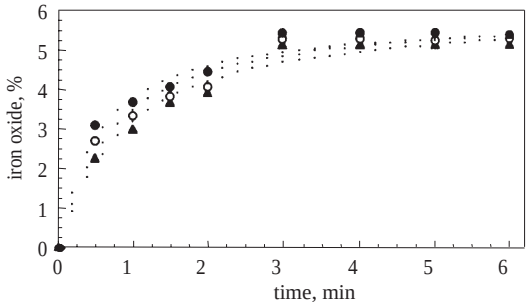

Figure 7b. The change in iron oxide solubility with USP and sonication time (for samples grain size 1 and mass 0.0500 g)
•; maximum USP, ◯ ; medium USP, ▲; minimum USP

The recoveries of Mn and Fe showed a linear increase for 30 minutes, which they remained constant with sonication time at all ultrasonic power.

Linear dissolution graphs 8a and 8b (t/S v t) were obtained, and r_i and S_{max} values plotted against ultrasonic power are shown in Figures 9a and 9b.

Both r_i and S_{max} values remained constant with ultrasonic power.

The effect of sample mass

The change in Mn and Fe solubilities of four equal samples for all grain sizes and sample masses at maximum ultrasonic power (that is, average values for 30-60 minutes sonication) are given in Figures 10a and 10b.

The solubilities decreased with increasing sample grain size for both elements. The maximum solubilities were observed for 0.0500 g sample mass and grain size 1. There was practically no residue, with only

0.0500 g of the sample portions remaining therefore, the recovery from these portions of samples must be equal to the value of that obtained by total dissolution.

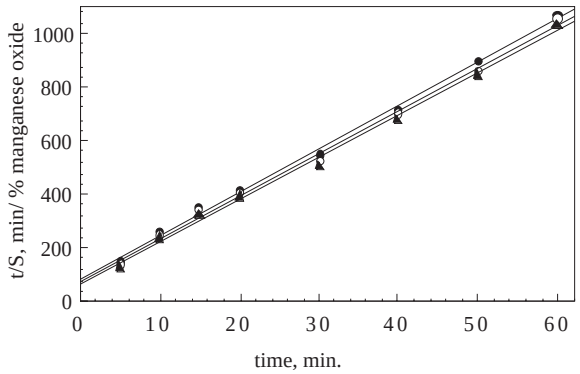

Figure 8a. t/S -t plot of manganese oxide (for grain size 1 and mass 0.0500 g)
•; maximum USP, ◯ ; medium USP, ▲; minimum USP

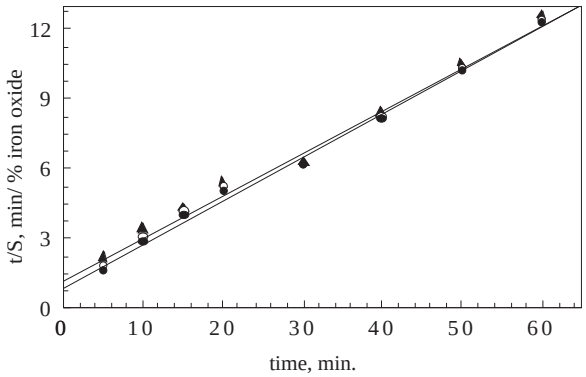

Figure 8b. t/S -t plot of iron oxide (for grain size 1 and mass 0.0500 g)
•; maximum USP,◯ ; medium USP, ▲; minimum USP

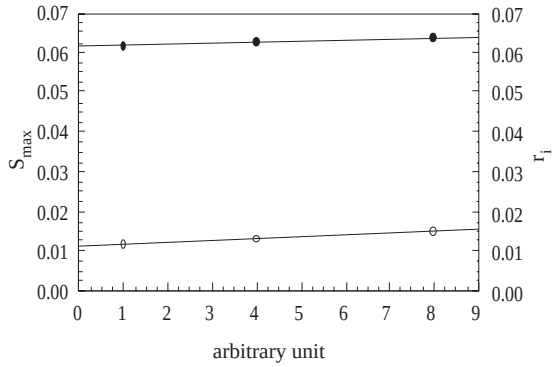

Figure 9a. The change in the values of S_{max} and r_i of manganese oxide with USP (for grain size 1 and mass 0.0500 g)
•; S_{max}(% manganese oxide / g sample), ◯; r_i(% manganese oxide /min g sample)

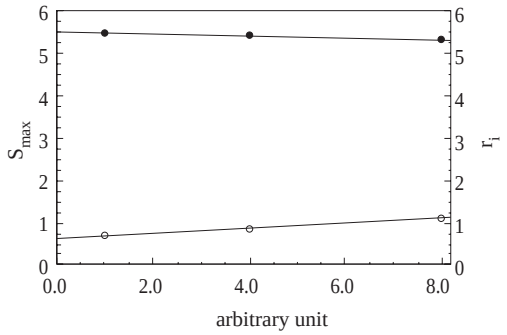

Figure 9b. The change in the values of S_{max} and r_i of iron oxide with USP (for grain size 1 and mass 0.0500 g)
•; S_{max}(% iron oxide / g sample), ◯; r_i(% iron oxide /min g sample)

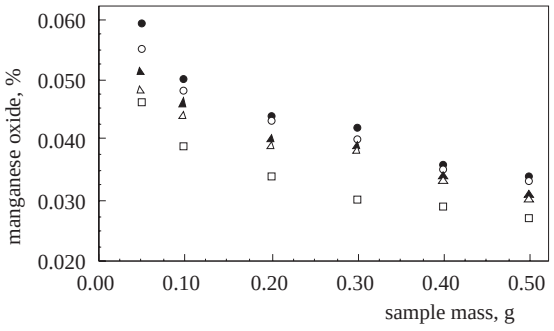

Figure 10a. The change in manganese oxide solubility with sample grain size and sample masses (maximum USP and mean values from 30 to 60 min)
•; grain size 1., ◯; grain size 2., ▲; grain size 3., Δ; grain size 4., ■; grain size 5.

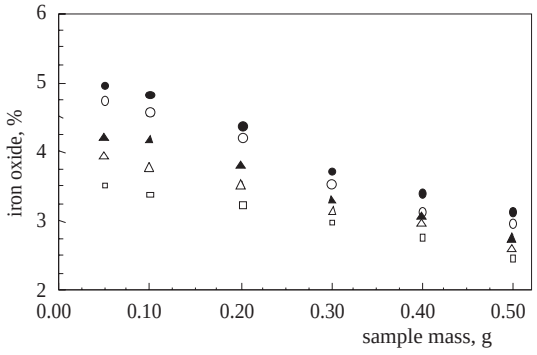

Figure 10b. The change in iron oxide solubility with sample grain size and sample masses (maximum USP and mean values from 30 to 60 min)
•; grain size 1., ◯; grain size 2., ▲; grain size 3., Δ; grain size 4., ■; grain size 5.

The solubilities of Mn and Fe for grain size 1 and all sample masses at varied ultrasonic power (minimum, medium and maximum) were investigated, and the findings are shown in Figures 11a and 11b respectively.

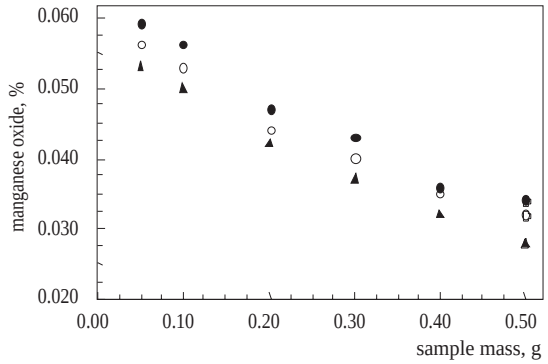

Figure 11a. The change in Mn solubility with sample mass and USP (grain size 1 and mean values from 30 to 60 min)
•; maximum USP, ◯; medium USP, ▲; minimum USP
USP

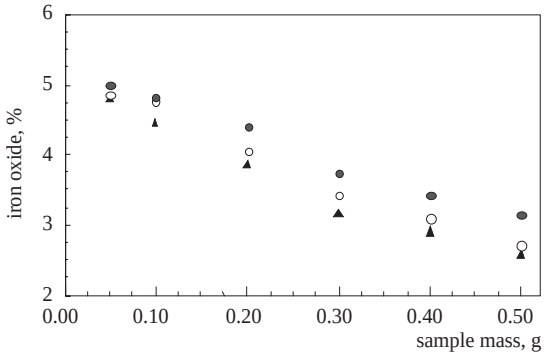

Figure 11b. The change in Fe solubility with sample mass and USP (grain size 1 and mean values from 30 to 60 min)
•; maximum USP,◯ ; medium USP, ▲; minimum USP

The solubilities of Mn and Fe rapidly decreased with increasing sample mass, and the recoveries were dependent upon USP. The trend was similar for other sample grain size.

The effect of sample grain size

The grain size has been previously defined (see Table 1) as the sieve pore size range. The effects of sieve pore size range and sample mass on the solubilities of Mn and Fe for all sample masses at maximum USP are given in Figures 12a and 12b.

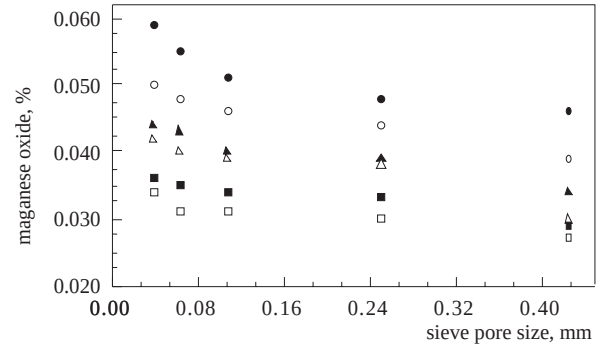

Figure 12a. The change in manganese oxide solubility with sieve pore size and sample masses (for maximum USP and mean values from 30 to 60 min)
•; 0.0500 g, ◯; 0.1000 g, ▲; 0.2000 g, Δ; 0.3000 g, ■; 0.4000 g, □; 0.5000 g,

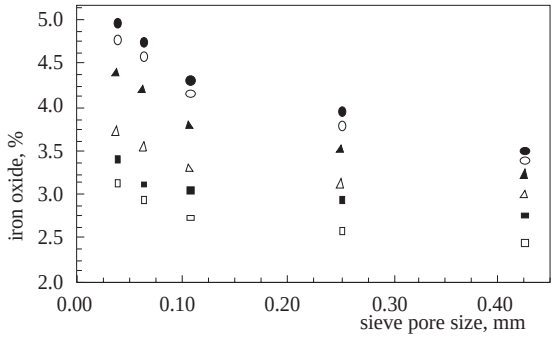

Figure 12b. The change in iron oxide solubility with sieve pore size and sample masses (for maximum USP and mean values from 30 to 60 min)
•; 0.0500 g, ◯; 0.1000 g, ▲; 0.2000 g, Δ; 0.3000 g, ■; 0.4000 g, □; 0.5000 g,

The maximum solubilities were obtained for 0.000-0.038 mm (grain size 1) sieve pore range and samples with 0.0500 g mass. The solubilities decreased up to 0.0106 mm rapidly, and then solubility rate slowed down with increasing grain size. In other words, the solubilities of Mn and Fe decreased with increasing

sample grain size. In all of the above mentioned conditions, the minimum sample grain size produced results equal to those of total dissolution for maximum USP. The situation is similar to those at other USPs.

The effect of ultrasonic power

The change in solubility with USP is shown in Figures 13a and 13b for Mn and Fe respectively.

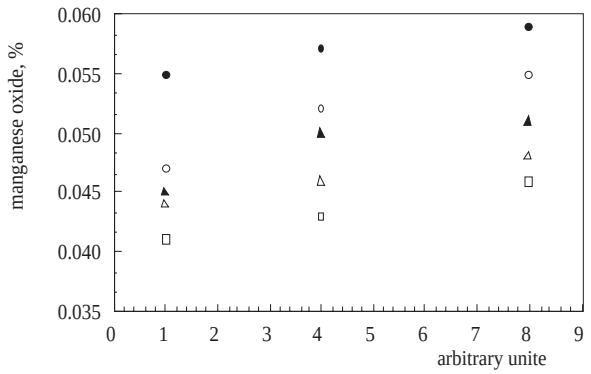

Figure 13a. The change in manganese oxide solubility with USP and grain size (for 0.0500 g sample, mean value from 30 to 60 min)
•; grain size 1., ◯; grain size 2., ▲; grain size 3., Δ; grain size 4., ■; grain size 5.

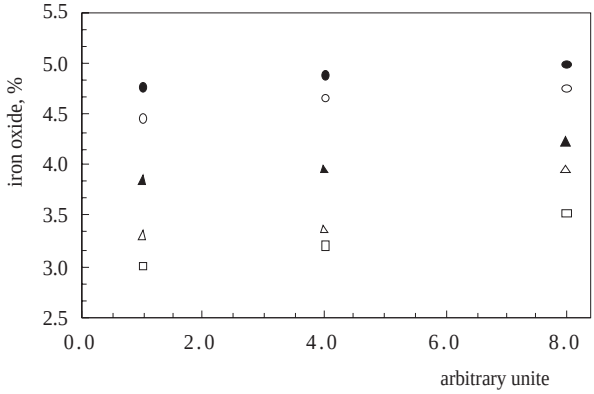

Figure 13b. The change in iron oxide solubility with USP and grain size (for 0.0500 g sample, mean value from 30 to 60 min)
•; grain size 1., ◯; grain size 2., ▲; grain size 3., Δ; grain size 4., ■; grain size 5.

While the solubility increased with increasing USP, it decreased with increasing sample grain size. The maximum recovery was obtained with maximum USP and grain size 1 (0.0000-0.0038 mm). The results from other sample masses confirmed this trend.

Evaluation of the solubilities of Mn and Fe

The solubility of both elements under all conditions exhibited a linear increase for the first 30 minutes and remained constant under all conditions studied. But the solubilities changed significantly, allowing us to determine the optimal conditions. Therefore the solubilities at 30, 40, 50 and 60 minutes of sonication time were evaluated as four equal samples. Maximum Mn and Fe solubilities were obtained with grain size 1, 0.0500 g sample mass and max USP (considered the optimum conditions). In fact, under these circumstances, practically no residual sample was left with ULM.

The results of ULM (C_{ULM}) were 0.058 and 4.98 in terms of percent metal oxide in the optimum conditions for Mn and Fe respectively.

The results of the conventional dissolution method[29](C_{CDM}) were 0.051 and 4.86 in terms of percent metal oxide for Mn and Fe respectively.

The confidence intervals were ± 0.003 and ± 0.07 for Mn and Fe (P=0.05 and N=4).

When the concentrations of Mn and Fe obtained from ULM at optimum conditions are compared to those of the conventional method, there was no significant difference between the results.

The amounts of residues increased with increasing sample mass and grain size, and hence the solubilities of Mn and Fe decreased. In spite of this handicap, reproducible partial dissolution was obtained in 30 minutes and during sonication time.

Average Mn and Fe solubilities which give reproducible results at five different grain sizes and six different sample masses were defined as follows for applied ultrasonic power:

$\bar{x}$ min USP: average as percentage of four repeated equal measurements at min USP

$\bar{x}$ med USP: average as percentage of four repeated equal measurements at med. USP

$\bar{x}$ min USP: average as percentage of four repeated equal measurements at max USP

Table 7. Solubilty and recovery manganese oxides, as percentages, obtained from different experimental conditions ($\bar{x}$ = Mean values of solubility from 30 to 60 minutes)
The indices min USP, med. USP and max USP correspond to USP.

Grain size	Sample mass, g	$\bar{x}^b_{\text{min USP}}$	K^b_{min}	$\bar{x}$med.USP[a]	$K^b_{med.}$	$\bar{x}$max USP[a]	K^b_{max}
1	0.0500	0.055	107.8	0.057	111.2	0.058	113.7
1	0.1000	0.048	94.1	0.051	100.0	0.052	101.9
1	0.2000	0.043	84.3	0.044	86.3	0.045	88.2
1	0.3000	0.037	62.3	0.039	76.5	0.041	80.4
1	0.4000	0.032	62.7	0.035	68.6	0.036	70.6
1	0.5000	0.028	54.9	0.031	60.9	0.034	66.7
2	0.0500	0.047	92.2	0.051	100.0	0.055	107.8
2	0.1000	0.045	88.2	0.046	90.2	0.048	94.1
2	0.2000	0.039	76.5	0.041	80.4	0.044	86.3
2	0.3000	0.034	66.7	0.036	70.6	0.040	78.4
2	0.4000	0.023	45.1	0.025	49.0	0.034	66.7
2	0.5000	0.021	41.2	0.023	45.1	0.033	64.7
3	0.0500	0.049	96.1	0.050	98.0	0.052	101.9
3	0.1000	0.046	90.2	0.047	92.2	0.048	94.1
3	0.2000	0.043	84.3	0.044	86.3	0.045	88.2
3	0.3000	0.036	70.6	0.039	76.5	0.040	78.4
3	0.4000	0.032	62.7	0.033	64.7	0.034	66.7
3	0.5000	0.029	56.9	0.030	58.8	0.031	60.9
4	0.0500	0.045	88.2	0.046	90.2	0.047	92.2
4	0.1000	0.041	80.4	0.042	82.4	0.045	88.2
4	0.2000	0.038	74.5	0.042	82.4	0.043	84.3
4	0.3000	0.036	70.6	0.040	78.4	0.041	80.4
4	0.4000	0.030	58.8	0.031	60.8	0.033	64.7
4	0.5000	0.029	56.9	0.031	60.8	0.032	62.7
5	0.0500	0.042	82.3	0.043	84.3	0.046	90.2
5	0.1000	0.035	68.6	0.039	76.5	0.040	78.4
5	0.2000	0.029	56.9	0.032	62.7	0.034	66.7
5	0.3000	0.027	52.9	0.029	56.9	0.030	58.8
5	0.4000	0.027	52.9	0.028	54.9	0.029	56.9
5	0.5000	0.026	50.9	0.028	54.9	0.029	56.9

a) Pooled standard deviation (σ) = 0.002 for N = 48 and degree of freedom =34

b) Percentage confidence interval = ± 0.2 (P=0.05 and N=4)

The percentage recovery ratio for the oxides of Mn and Fe were derived from

Kmin: $\bar{x}_{minUSP}/C_{CDM}$ x100,

Kmed: $\bar{x}_{medUSP}/\mathrm{C}_{CDM}$ x100 and

Kmax: $\bar{x}_{\max USP}/\mathrm{C}_{CDM}$ x100.

The percentage recovery ratios found depending on applied USP for five different grain sizes and six sample mass are provided in Tables 7 and 8 respectively.

Recovery rates were 50.9 (for grain size 5, 0.5000 g sample mass and minimum USP)-113.7 (for optimum conditions) % for Mn and 37.0 (for grain size 5, 0.5000 g sample mass and minimum USP) -102.5 (for optimum conditions) for Fe.

Table 8. Solubility and recovery iron oxides, as percentages, obtained from different experimental conditions ($\bar{x}$ = Mean values of solubility from 30 to 60 minutes)
The indices min USP, med. USP and max USP correspond to USP.

Grain size	Sample mass, g	$\bar{x}^{b}_{\min\,\mathrm{USP}}$	$\mathrm{K}^{b}_{\min}$	$\bar{x}$med.USP[a]	$\mathrm{K}^{b}_{med.}$	$\bar{x}$max USP[a]	$\mathrm{K}^{b}_{\max}$
1	0.0500	4.76	97.9	4.86	100.0	4.98	102.5
1	0.1000	4.46	91.8	4.81	98.9	4.82	99.2
1	0.2000	3.71	76.3	4.05	83.3	4.40	90.5
1	0.3000	3.18	65.4	3.42	70.4	3.73	76.7
1	0.4000	3.01	61.9	3.10	63.8	3.43	70.6
1	0.5000	2.57	52.9	2.71	55.8	2.97	61.1
2	0.0500	4.46	91.8	4.67	96.1	4.76	97.9
2	0.1000	4.29	88.3	4.48	92.2	4.59	94.4
2	0.2000	3.83	78.8	3.94	81.1	4.19	86.2
2	0.3000	3.09	63.6	3.30	67.9	3.55	73.0
2	0.4000	2.85	58.6	2.97	61.1	3.13	64.4
2	0.5000	2.37	48.8	2.54	52.3	2.96	60.9
3	0.0500	3.84	79.0	3.94	81.1	4.22	86.8
3	0.1000	3.75	77.2	3.82	78.6	4.18	86.0
3	0.2000	3.49	71.8	3.69	75.9	3.80	78.2
3	0.3000	2.97	61.1	3.21	66.0	3.30	67.9
3	0.4000	2.58	53.1	2.83	58.2	3.07	63.2
3	0.5000	2.19	45.1	2.38	48.9	2.76	56.9
4	0.0500	3.31	68.1	3.35	68.9	3.95	81.3
4	0.1000	3.07	63.2	3.26	67.1	3.79	77.9
4	0.2000	2.89	59.5	3.12	64.1	3.54	72.8
4	0.3000	2.83	58.2	3.01	61.9	3.13	64.4
4	0.4000	2.56	52.7	2.71	55.8	2.96	60.9
4	0.5000	2.12	43.6	2.24	46.1	2.61	53.7
5	0.0500	3.01	61.9	3.21	66.0	3.52	72.4
5	0.1000	2.81	57.8	3.10	63.8	3.39	69.8
5	0.2000	2.33	47.9	2.87	59.1	3.25	66.9
5	0.3000	2.22	45.8	2.58	53.1	2.99	61.5
5	0.4000	2.01	41.4	2.58	53.1	2.78	57.2
5	0.5000	1.80	37.0	2.12	43.6	2.46	50.6

a) Pooled standard deviation (σ) = 0.05 for N = 48 and degree of freedom =34

b) Percentage confidence interval = ± 4.9 (P=0.05 and N=4)

The results of SRM

Validation of the developed method was conducted by using standard reference materials (SRM). Values of elemental concentrations (C_{SRM}) were obtained from the certificates of analysis or from the compilation of usable values by Govindaraju[29]. The SRM were used in this study as follows:

Table 9. The manganese oxide % values of SRM and the recovery ratios

SRM	C_{SRM}	C^a_{ULM}	K_1 $(C_{ULM}/C_{SRM})^b$	C^a_{CDM}	K_2 $(C_{ULM}/C_{CDM})^b$
AGV-1	0.092	0.084	91.3	0.087	96.6
G-2	0.032	0.030	93.8	0.031	96.8
RGM-1	0.036	0.035	97.2	0.036	97.2
SDC-1	0.114	0.118	103.5	0.120	98.3
GA	0.090	0.085	94.4	0.092	92.4
GH	0.050	0.051	102.0	0.048	106.3
Mica Fe	0.350	0.330	94.3	0.360	91.7
DRN	0.220	0.240	109.1	0.220	109.1
GSN	0.056	0.052	92.9	0.054	96.3
MA-N	0.040	0.042	105.0	0.039	107.7
AC-E	0.058	0.055	94.8	0.058	94.8
Mica-Mg	0.026	0.024	92.3	0.027	88.9
UBN	0.120	0.127	105.8	0.125	101.6
ANG	0.040	0.038	95.0	0.040	95.0
BEN	0.200	0.196	98.0	0.207	94.7

a) Pooled standard deviation (σ) = 0.002 for N = 60 and degree of freedom =45
b) Percentage confidence interval = ± 0.2 (P=0.05 and N=4)

Table 10. The iron oxide percentage values of CRM and the recovery ratios

SRM	C_{SRM}	C^a_{ULM}	K_1 $(C_{ULM}/C_{SRM})^b$	C^a_{CDM}	K_2 $(C_{ULM}/C_{CDM})^b$
AGV-1	6.76	6.43	95.1	6.50	98.9
G-2	2.66	2.63	98.9	2.45	107.3
RGM-1	1.86	1.65	88.7	1.80	91.7
SDC-1	6.90	6.72	97.4	6.50	103.4
GA	2.83	2.58	91.2	2.65	97.4
GH	1.34	1.30	97.0	1.24	104.8
Mica Fe	25.655	22.12	86.2	23.14	95.6
DRN	9.70	9.21	94.9	9.05	101.7
GSN	3.75	3.60	96.0	3.50	102.9
MA-N	0.47	0.45	95.7	0.45	100.0
AC-E	2.53	2.35	92.9	2.45	104.3
Mica-Mg	9.46	9.11	96.3	9.68	94.1
UBN	8.34	7.85	94.1	7.90	99.4
ANG	3.36	3.00	89.3	3.07	97.7
BEN	12.84	11.51	89.6	12.15	94.7

a) Pooled standard deviation (σ) = 0.040 for N = 60 and degree of freedom = 45
b) Percentage confidence interval = ± 3.9 (P=0.05 and N=4)
c) Pooled standard deviation (σ) = 0.036 for N = 60 and degree of freedom = 45
d) Percentage confidence interval = ± 3.5 (P=0.05 and N=4).

USGS (AGV-1, G-2, RGM-1 and SDC-1), CRPG (GA, GH, MICA-Fe and MICA-Mg), ANRT (DRN, GSN and UB-N) and GIT-IWG (MA-N, AC-E, AN-G and BE-N).

The SRM were leached under the optimised ULM conditions, and the conventional method and experiments were repeated four times. All leachates are analysed using an AAS and results are given in Tables 9 and 10 for Mn and Fe as an average percentage including recovery rate percentage. K_1: C_{ULM}/C_{SRM} x100 and K_2: C_{ULM}/C_{CDM} x100

Recovery rates were 88.9-109.1% for Mn and 86.2-107.3 for Fe.

Conclusions

Reproducible element recovery ratios were obtained in well defined partial dissolution conditions. Similar results were obtained for both elements investigated; therefore, it seemed that the situation does not depend upon the nature of the element.

The confidence interval of the method is comparable with those of conventional techniques. Clearly, the method is quicker than the conventional counterparts. The reagent consumption of the method is less than that of the total dissolution methods and hence the method is environmentally friendly.

The method can be offered as a speedy, inexpensive, reproducible and harmless alternative dissolution process if it is supported by complementary investigations.

Acknowledgements

We are grateful to Dr. M. Sökmen and Dr. D. Saraydın, at the Department of Chemistry, and Dr. Durmuş Boztuğ, at the Department of Geology of Cumhuriyet University, for their assistance.

References

1. F.C. Hawthorne, **Spectroscopic Methods in Mineralogy and Geology**, Book Crafters, Inc., Chelsea, Michigan (1988).
2. F. E. Lichte, J. L. Seely, L. L. Jackson, D. M. Mc Kown and J. E. Taggart, Jr., **Anal. Chem., 59**, 197R-212R (1987).
3. L. L. Jackson, D. M. Mc Kown and J. E. Taggart, Jr., P. J. Lamothe and F. E. Lichte, **Anal. Chem., 61**, 109R-128R (1989).
4. L. L. Jackson, T. L. Fries, J. N. Grosman, B. S. W. King and P. J. Lamothe, **Anal. Chem., 63**, 33R-48R (1991).
5. L. L. Jackson, P. A. Baedecker, T. L. Fries and P. J. Lamothe, **Anal. Chem., 65**, 12R-28R (1993).
6. A. G. Howard, P. J. Statham, **Inorganic Trace Analysis**, **Philosophy and Practice**, John Wiley and Sons Inc., New York (1997).
7. D. A. Skoog, D. M. West, F. J. Holler, **Analytical Chemistry**, Saunders College Pub, Philadelphia (1996).
8. Z. Zhang, M. J. Yang, J.Pawliszyn, **Anal. Chem**, **66**, 844-853A (1994).
9. A. D. Pandey, K. Mallick, P. C. Pandey, **Proct. Int. Cong., 2**,463-72 (1980).

10. P. Bowdjouk, **J. Chem. Educ.**, **63**, 427-29 (1986).
11. C. Seghal, R. G. Sutherland, R. E. Verral, **J. Phys. Chem.**, **84**, 396 (1980).
12. T. K. Alben, H. J. Kaczmarczyk, **Anal. Chemy.**, **58**, 1817-22 (1986).
13. J. Grimalt, C. Morfil, J. Albages, **Intern. J. Environ. Anal. Chem.**, **18**, 183-94 (1984).
14. H. W. Griest, B. L. D. Yeatts, J. E. Caton, **Anal Chem**, **52**, 201-3 (1980).
15. T. S. Koh, **Anal. Chem., 55,** 1814-18 (1983).
16. S. L. Harper, J. F. Walling, D. M. Holland and L. J. Prongler, **Anal. Chem., 55,** 1553-57 (1983).
17. M. H. Özkan and M. Akçay, **35^{th} IUPAC Congress,2,** pp.127,14-19 August (1995).
18. M. H. Özkan and M. Akçay, **XIII. National Chem. Congress,** pp 103, 31 August (1999).
19. M. H. Özkan and M. Akçay, **3rd Mediterranean Basin Con. on Anal. Chem.**, pp. 140, 4-9 Jun (200).
20. A. Elik, M. Akçay, Ş. Savaşcı, **Tr J Chem.**, **15**, 130-139 (1991).
21. M. Akçay, A. Elik, Ş. Savaşcı, **Analyst, 114**, 1079-82 (1989).
22. A. Elik, M. Akçay, M. Sökmen, **Intern. J. Environ Anal. Chem.**, **77**, 133-145 (2000).
23. J. C. Miller, J. N. Miller, **Statistics For Analytical Chemistry,** John Wiley Sons Inc., New York (1988).
24. C. Peniche, M. A. Cohen, B. Vasquez and J. S. Roman, **Polymer**, **38**, 5977-5982 (1997).
25. I. Katime, J. L. Velada, R. Novoa and E. D. de Apodaca, **Polym. Int.**, **40**, 281-286 (1996).
26. N. Şahiner, D. Saraydın, E. Karadağ and O. Güven, **Polym. Bull.**, **41**, 371-378 (1998).
27. S. Yılmaz, D. Boztuğ, **Intern. Geology Review, 38,** 935-56 (1995).
28. L.D. Muller, **Laboratory Methods of of Mineral Separation.** In: J. Zussman (ed.), Physical Methods in Determinative Mineralogy, Academic Press, London, pp, 1- 34, (1977).
29. K. Govindaraju, **Geostandards Newsletter, 13**, 1-113 (1989).